ADVANCED ENERGY MATERIALS
www.advenergymat.de

Next-Generation Cobalt-Free Cathodes – A Prospective Solution to the Battery Industry's Cobalt Problem

Nitin Muralidharan,* Ethan C. Self, Marm Dixit, Zhijia Du, Rachid Essehli, Ruhul Amin, Jagjit Nanda, and Ilias Belharouak*

Lithium-ion batteries are overreliant on cobalt containing cathodes. Current projections estimate that hundreds of millions of electric vehicles (EVs) will be on road by 2050, and this ever-growing demand threatens to deplete global cobalt reserves at an alarming rate. Moreover, cobalt supply chain issues have significantly increased cobalt prices throughout the last decade. As such, energy storage research and development need to reduce reliance on cobalt to meet ever-growing demands for lithium-ion batteries. The present review summarizes the science and technology gaps and potential of numerous cobalt-free Li-ion cathodes including layered, spinel, olivine, and disordered rock-salt systems. Despite the promising performance of these Co-free cathodes, scale-up and manufacturing bottlenecks associated with these materials must also be addressed to enable widespread adoption in commercial batteries. Overall, this review broadly highlights the enormous promise of "zero-cobalt" Li-ion batteries to enable sustainable production of EVs in the coming decades.

1. Introduction

Market opportunities for Li-ion batteries (LIBs) are ever-growing beyond traditional consumer electronics to include electric vehicles (EVs) and grid storage applications.[1,2] Research and development (R&D) efforts by national laboratories, academia, and industry are largely focused on next-generation materials and chemistries to enable higher energy, higher power, and/or lower cost batteries. The goal of net zero carbon emissions has catalyzed the demand on EVs with projections of nearly 200 million vehicles on the road by the year 2050.[3,4] Within this ecosystem, industries that manufacture Li-ion batteries are projected to operate on profitability models hedged on economy of scale. While being the cornerstone to this global effort, battery manufacturing is increasingly challenged to secure a more resilient and sustainable material supply chain for decades to come.

Among those challenges, cobalt stands out as a key ingredient for cathode production and accounts for roughly 25–30% of the overall battery cost.[2] This situation will continue for the next several years, as the state-of-the art Li-ion battery technology is not yet ready to depart from cobalt-containing cathodes, such as $LiNi_{0.8}Co_{0.15}Al_{0.05}O_2$ (NCA) and $LiNi_xMn_yCo_{1-x-y}O_2$ (NMC). In recent years, cobalt prices have nearly tripled due to increased demand driven by supply chain constraints (**Figure 1**a), creating unpredictable scenarios for battery manufacturing. Today's cobalt price is nearly 60% higher than that of nickel, the latter being the second most critical element used in LIBs. In a recent report, the Cobalt Development Institute reported that roughly 40% of global cobalt production is directed toward LIBs, and the remaining 60% is geared toward wide range of applications including catalysts, magnets, super alloys, and pigments (Figure 1b).[5] These statistics highlight a scenario where limited availability of cobalt could hinder growth of the EV market.

The growth associated with the millions of EVs that are projected to be on the road by 2050 will outpace Co availability in the coming decades. Unless Co-free cathodes and/or recycling solutions are implemented for EV batteries, Co demand will exceed global cobalt reserves available for battery manufacturing before 2045 (Figure 1c) (this calculation uses metrics from known global cobalt reserves, ≈7 million metric ton total,[6,7] however, if we recompute assuming conservative mining efficiencies of ≈70% and cobalt directed toward battery manufacturing industries to be ≈40%, the total usable battery specific cobalt from the total reserves reduces to ≈2 million metric ton). This alarming scenario clearly illustrates that present-day LIBs are overreliant on cobalt as a critical resource. It is noteworthy to highlight the pivotal role that the U.S. Department of Energy played during the last two decades to reduce LIB cost by nearly eightfold with a goal to further reduce LIB cost to less than \$60 kWh^{-1} by 2030. This new goal requires lowering the cathode's cobalt content to less than 50 mg Wh^{-1} at the cell level along with other manufacturing cost reductions. If this goal becomes a reality, global battery manufacturers will need a few years to integrate these novel

N. Muralidharan, M. Dixit, Z. Du, R. Essehli, R. Amin, I. Belharouak
Electrification and Energy Infrastructures Division
Oak Ridge National Laboratory
Oak Ridge, TN 37831, USA
E-mail: muralidharan@ornl.gov; belharouaki@ornl.gov
E. C. Self, J. Nanda
Chemical Sciences Division
Oak Ridge National Laboratory
Oak Ridge, TN 37831, USA
The ORCID identification number(s) for the author(s) of this article can be found under https://doi.org/10.1002/aenm.202103050.

DOI: 10.1002/aenm.202103050

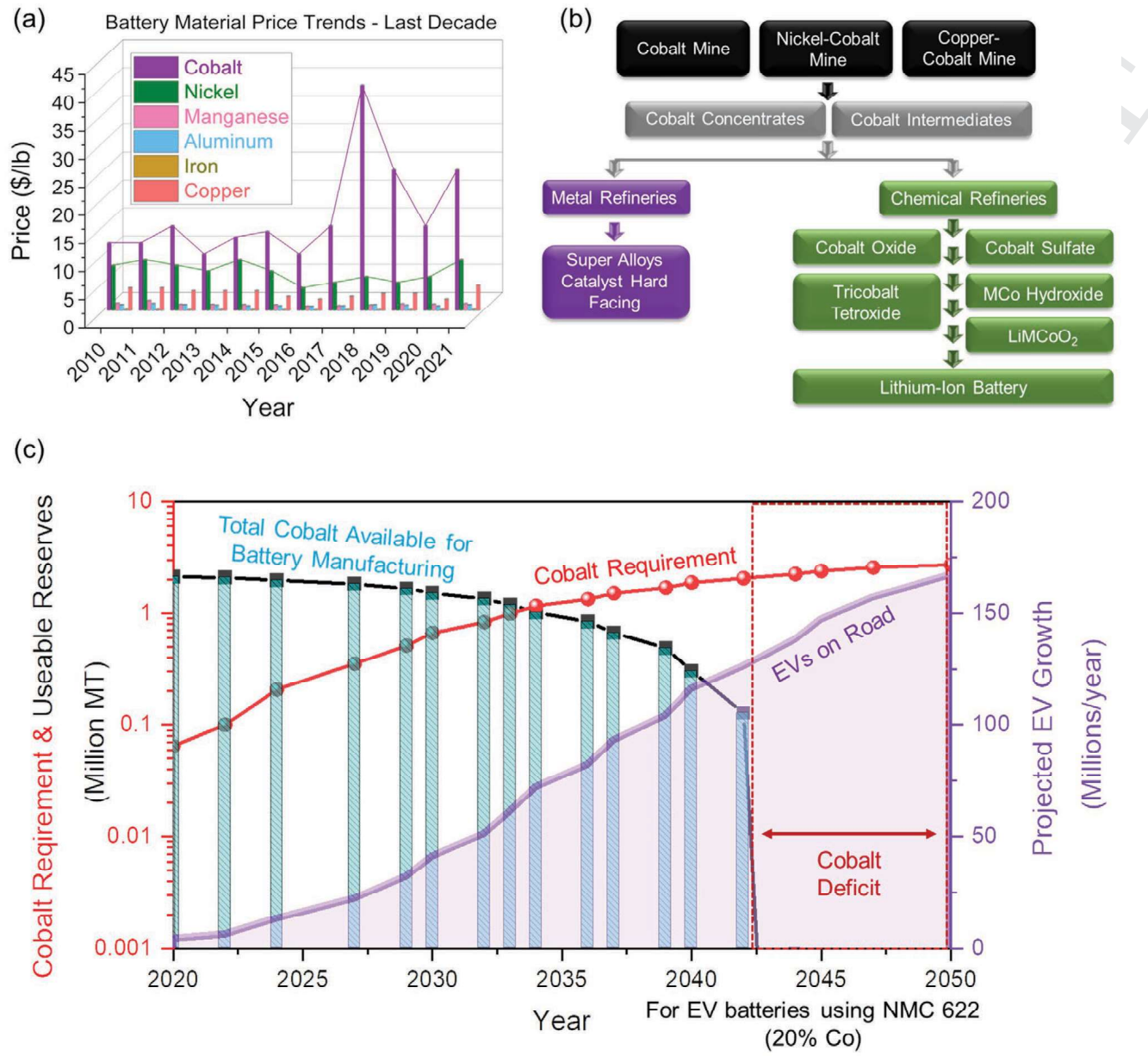

Figure 1. a) Battery material price trends from 2010 to 2021. b) Market flow chart for cobalt. c) Model highlighting the depletion of global cobalt reserves specifically available for battery industries, leading to a shortage of cobalt based on the projected number of electric vehicles on road in the first half of the 21st century. In our calculation, we use the total global cobalt reserves obtained from USGS 2021 report on cobalt[7] (7 million metric tons) and assume a conservative ≈70% yearly mining efficiency with ≈40% of the mined cobalt directed toward battery manufacturing. Our recomputed estimate for the total cobalt available for battery industries considering all these parameters is ≈2 million metric tons globally.

cathode compositions without undergoing substantial overhauls. Indeed, any new low-Co or Co-free cathodes should be designed such that they are compatible with existing global battery manufacturing infrastructures.

The present review highlights recent developments on advanced low-Co/Co-free cathodes for LIBs. The review specifically discusses the performance of layered, spinel, olivine, and disordered rock-salt (DRX) cathodes and the challenges related to upscaling and manufacturing of these materials. Overall, the review aims to provide a comprehensive overview of technical hurdles while highlighting the potential of low-Co/Co-free cathodes for next-generation LIBs.

2. Market Potential of Cobalt-Free Cathodes

To meet the LIB requirements for the projected EV market in the coming decades, widespread adoption of high-performance low-Co/Co-free cathodes is essential. This point is illustrated here where we consider the battery cost to produce one million EVs (200 mile range) powered by 58.8 kWh LIB packs where the cathode includes either: i) commercially available Co-based cathodes (i.e., NMC111, NMC622, or NCA) and ii) Co-free cathodes such as $LiNiO_2$, $LiNi_xMn_yAl_{1-x-y}O_2$, and $LiNi_xFe_yAl_{1-x-y}O_2$ (NFA). These calculations were performed using the Argonne National Laboratory's BatPac battery design and cost model.[8]

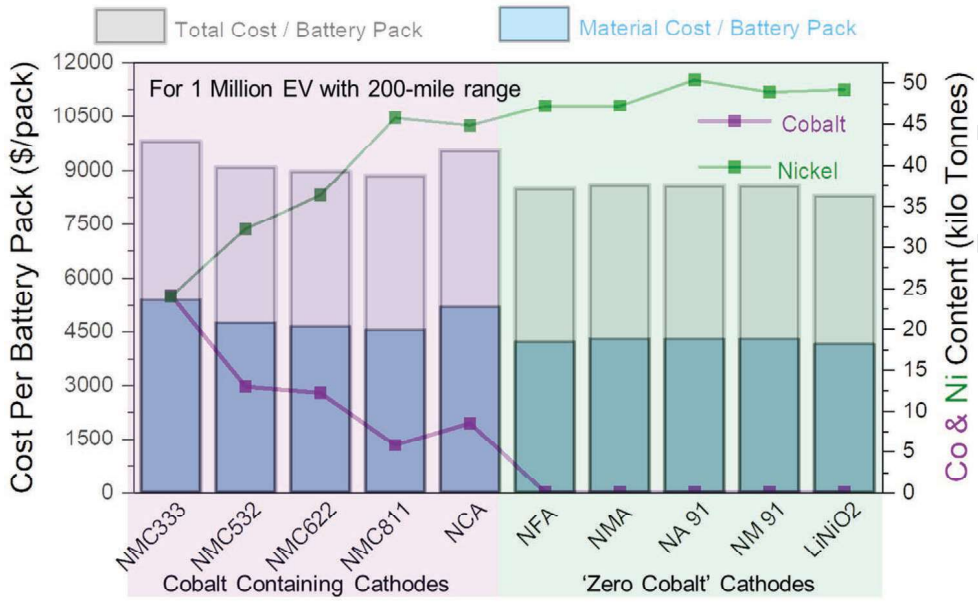

Figure 2. Potential of Co-free cathode materials for low-cost LIBs. Cost projections are based on producing 1 million EVs with a 200 mile range powered by 58.8 kWh LIB packs.

For example, if NCA cathodes are utilized, nearly 10 kilotons of cobalt are needed to produce 1 million EVs (**Figure 2**). Likewise, producing >150 million EVs by 2050 using NMC622 cathodes would require more than 2.5 million metric tons of usable cobalt which represents more than one third of the known global Co reserves (≈7 million metric tons[7]). Thus, Co-heavy cathodes are unable to meet future EV demands, and it is unrealistic to expect the battery manufacturers would offset the high cost of cobalt in a constrained supply chain market. Transitioning to cobalt-free chemistries is the most straightforward pathway to meet skyrocketing demand for affordable EVs in the coming decades. The analysis in Figure 2 anticipates that the adoption of Co-free cathodes will significantly reduce battery costs ($8500 total pack cost, $3500 material costs) compared to a battery system containing NCA cathodes ($10 000 total pack cost, $5000 material cost).

Clearly, cathode selection has the most impact on LIB cost and performance. To enable widespread adoption of low-Co/Co-free cathodes for EV applications, a comprehensive understanding of challenges related to cathode performance and manufacturing is needed. The following sections discuss these issues for several promising low-Co/Co-free cathodes including layered, spinel, olivine, and DRX systems.[2,9,10] The structure and representative voltage profiles for such cathodes are represented in **Figure 3**.

3. Layered Oxide Cathodes

3.1. Conventional Layered Cathodes

Lithium cobalt oxide ($LiCoO_2$, LCO) with a layered rhombohedral structure (space group $R\bar{3}m$) was used in the first commercial LIBs and continues to be used in several consumer electronics today. LCO has a high theoretical capacity of 274 mAh g^{-1}, although typically only ≈140 mAh g^{-1} is available for practical applications (Figure 3). Furthermore, the high cost and toxicity associated with Co led the battery community to pursue a comparatively low-cost layered lithium nickel oxide ($LiNiO_2$ or LNO: theoretical capacity ≈ 275 mAh g^{-1}) as an alternative. However, LNO is a difficult material to synthesize, and it also suffers from detrimental structural transitions, resulting in poor cycling performance. Additionally, LNO also suffers from cation mixing issues wherein some of the Li^+ and Ni^{2+} ions exchange positions in the crystal structure. Formation of these defects creates ion diffusion bottlenecks that result in low capacities and poor cycling stability. To overcome these limitations, several metal substitutions/dopants including aluminum, cobalt, and/or manganese were extensively investigated to improve LNO's stability and electrochemical performance.[12,13] For example, partial substitution of Ni with Co, Mn, and/or Al in commercial NCA ($LiNi_xCo_yAl_{1-x-y}O_2$) and NMC cathodes has been shown to stabilize the layered structure while suppressing O_2 gas evolution and thermal runaway. The characteristics and benefits of layered cathodes with one or more transition metal substitutions are discussed in the next paragraphs.

3.2. Binary Layered Ni-Rich Cathode Materials

Most common binary cathode chemistries ($LiM_{Ix}M_{IIy}O_2$, where $x + y = 1$ and M_I, M_{II} are metal ions) have been centered around nickel-rich compositions with either manganese or aluminum substitutions/dopants. Particularly, manganese substitutions in LNO system have gained significant interest in recent times. Mn doping has been shown to enhance the thermal stability of nickel containing cathode structures especially in their delithiated states. The tetravalent Mn^{4+} ions are usually inactive electrochemically and are thus considered to mitigate the Jahn–Teller distortions plaguing the LNO crystal structure during

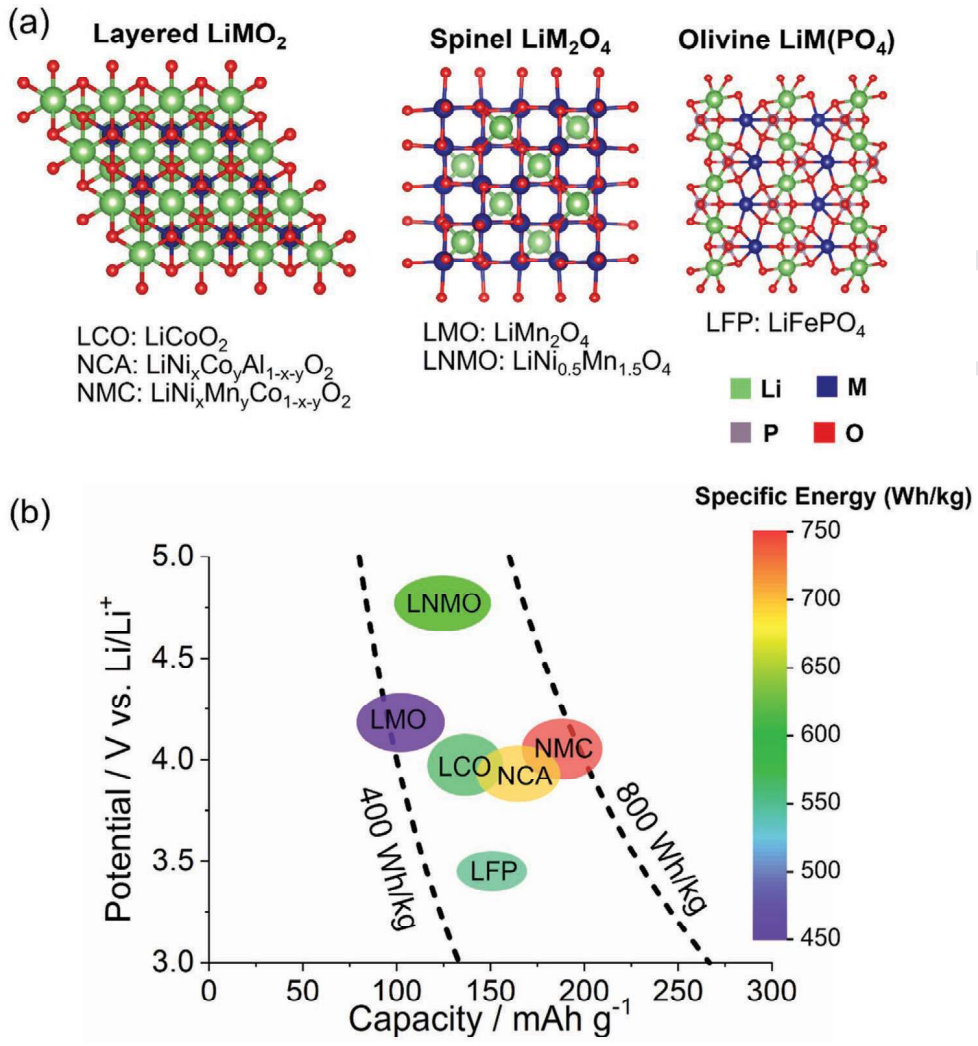

Figure 3. a) Crystal structures of mainstream Li-ion cathodes such as layered ($R\bar{3}m$), spinel (*Fd*–3*m*), and olivine (*Pnma*) systems (viewed along the *a*-axis). Crystallographic structures were generated using VESTA software.[11] b) Operating potential, specific capacity, and specific energy of several such cathodes.

delithiation/lithiation cycles. Prior studies have reported the cycling and thermal stability benefits achieved through the incorporation of Mn atoms in LNO systems in a wide range of compositions including $LiNi_{0.5}Mn_{0.5}O_2$ and $LiNi_{0.9}Mn_{0.1}O_2$. The systematic investigations of Mn-doped LNO systems by Sun et al.[14] ($LiNi_\gamma Mn_{1-\gamma}O_2$, between $0.5 \leq \gamma \leq 0.9$) are shown in **Figure 4**.

Figure 4a,b shows galvanostatic charge/discharge profiles and cycling performance of Co-free Mn-substituted LNO. Increasing the Mn content improves cycling stability at the expense of discharge capacities, (e.g., 212 mAh g^{-1} (10% Mn) vs 164 mAh g^{-1} (50% Mn)), owing to the electrochemical inactivity of Mn^{4+} ions. Figure 4c,d shows the reported thermal stabilities of the Mn-doped LNO electrodes in their delithiated states. Cathode systems with lower Mn content generated comparatively less heat during thermal decomposition tests (901.4 J g^{-1} for 10% Mn vs 485.7 J g^{-1} for 50% Mn). It was speculated that spinel phase formation improved structural integrity of the 10% Mn-doped LNO sample and delayed the onset of exothermic reactions.

Mg and Al substitutions have been widely reported to improve the electrochemical performance of LNO cathodes.[15] Mg substitutions have been shown to improve cycling stability by mitigating cathode particle cracking during Li insertion/extraction. Li et al.[16] reported the systematic investigation of Al ($LiNi_{0.9}Al_{0.1}O_2$)-, Mg ($LiNi_{0.9}Mg_{0.1}O_2$)-, Co ($LiNi_{0.95}Co_{0.05}O_2$)-, and Mn ($LiNi_{0.9}Mn_{0.1}O_2$)-doped LNO systems (**Figure 5**a–c). Based on the differential capacity plots shown in Figure 5a, the authors concluded that by adding Al, Mn, and Mg ions to the transition metal layer, the LNO cathodes suppressed detrimental phase transitions during delithiation/lithiation.

The authors also reported that Mn, Mg, and Al substitutions improved the thermal stability when compared to undoped LNO (Figure 5b). While delithiated LNO with/without 5% Co dopant exhibited thermal runaway at temperatures > 160 °C, delithiated LNO doped with 5% Al, Mg, and Mn did not reach the threshold self-heating rate under the same testing conditions. These results demonstrate how these dopants can stabilize layered LNO systems in their delithiated states.

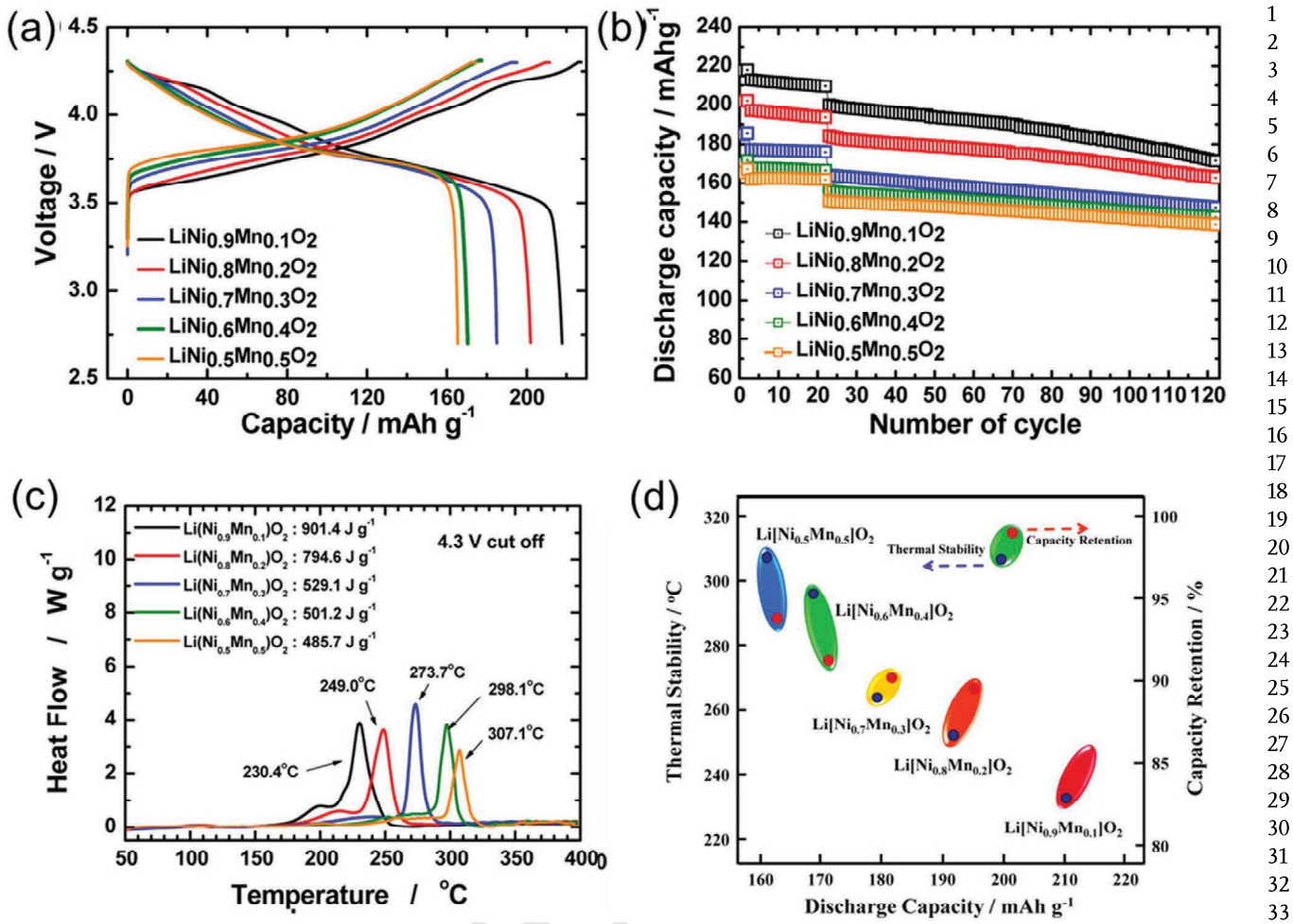

Figure 4. Electrochemical and thermal performance of Mn-substituted LNO cathodes. a) Galvanostatic charge/discharge profiles, b) cycling stability, c) heat flow profiles of delithiated electrodes, d) thermal stability as a function of discharge capacity for several cathodes. Adapted with permission.[14] Copyright 2013, American Chemical Society.

Electrochemical performance assessment of the Al-, Mn-, and Mg-doped LNO systems (Figure 5c) revealed better capacity retention for the Al–LNO binary nickel-rich cathode when compared to NCA containing 15% Co. Nevertheless, despite the promising results reported in literature for binary cobalt-free nickel-rich layered cathodes, scalability-, processibility-, and safety-related challenges limit their practical viability at present, thus warranting further investigations.

3.3. Ternary Layered Ni-Rich Cathode Materials

The quest for developing cobalt-free analogs of commercially available NCA and NMC is increasingly gaining momentum due to cobalt supply chain issues discussed previously. The primary motivation for developing such cathode systems stems from the hypothesis that multiple metal ion additions are expected to resolve several issues simultaneously (e.g., thermal stabilities, capacity fade, reduction in cation mixing, etc.). In line with this hypothesis, our team has been actively pursuing several R&D thrusts on development and scale-up of ternary cobalt-free nickel-rich cathode formulations including the iron containing $LiNi_xFe_yAl_zO_2$ (NFA where, $x \geq 0.8$, $x + y + z = 1$).[17,18] Our team's approach is primarily motivated by the premise that high nickel content yields high capacities which can be coupled with improved electrochemical performance by replacing some of the nickel cations with small amounts of trivalent iron and aluminum. These elements were chosen specifically due to their similar ionic radii to Ni^{3+} (0.54 Å for Al^{3+} and 0.55 Å for Fe^{3+} compared to 0.56 Å for Ni^{3+}). These dopant additions are expected to enhance the structural stability, reduce cation disorder, improve safety, and deliver long cycle life. A schematic depicting the benefits of iron and aluminum incorporation and the resulting crystal structure is shown in **Figure 6**a. Neutron diffractograms of NFA cathode compositional variants showing a rhombohedral crystal structure, with $R\bar{3}m$ space group, corresponding to α-$NaFeO_2$ crystal structure are shown in Figure 6b. As discussed earlier, it is expected that nickel-rich cathode structures suffer from cation mixing challenges due to the similar ionic radii of Ni^{2+} and Li^{+}. Using Rietveld refinement and analysis of the neutron diffractograms, we determined that the antisite defect formation was only ≈4% in NFA cathode variants.

The NFA cathode materials were also upscaled from bench scale to kilogram levels using a coprecipitation synthesis route.

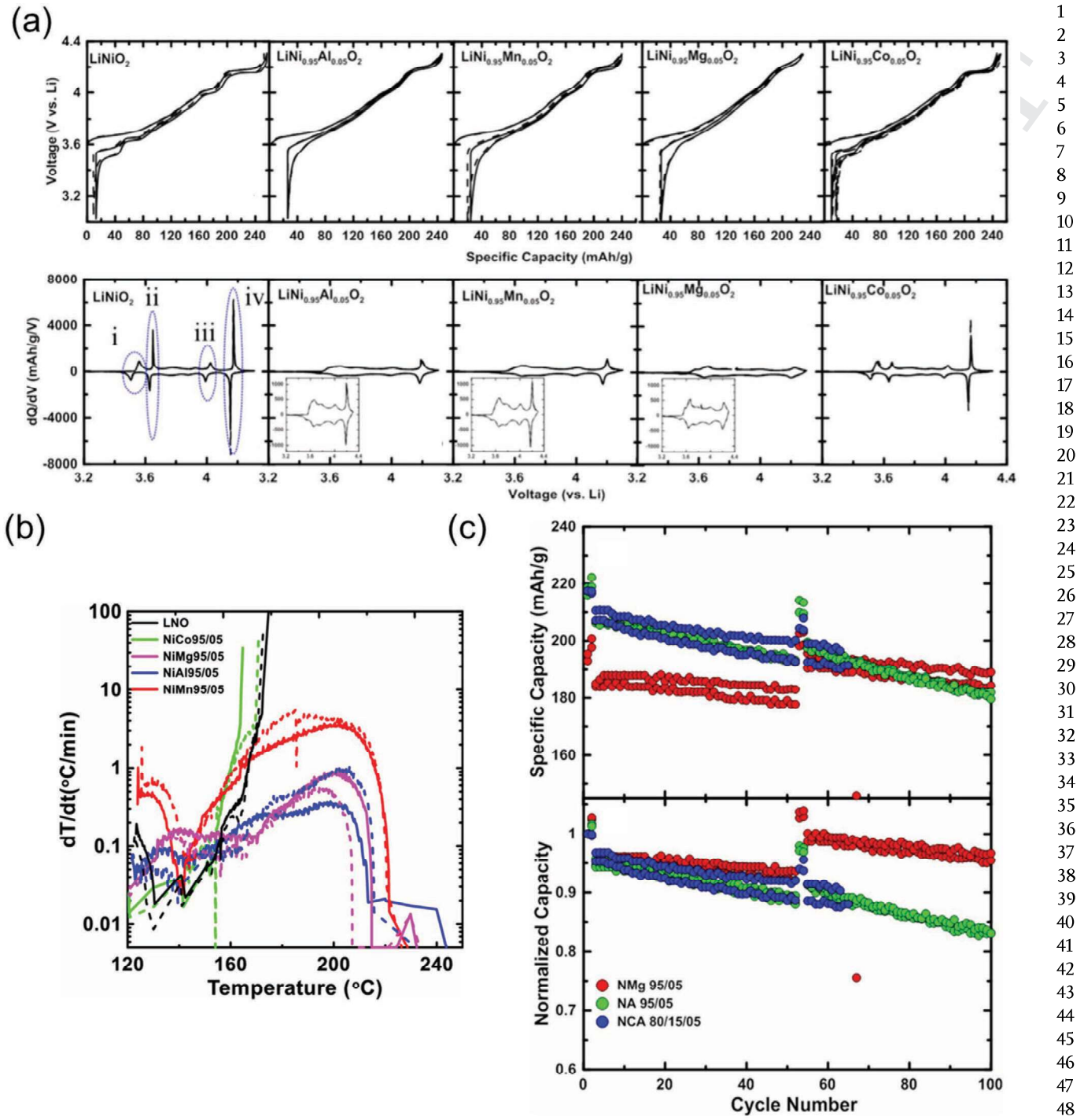

Figure 5. a) Galvanostatic charge/discharge plots (top) and dQ/dV profiles (bottom) for several doped LNO systems. b) Thermal stabilities of doped LNO systems determined through accelerated rate calorimetry tests. c) Electrochemical performance of doped LNO systems compared to commercial NCA cathodes. Adapted under the terms of the creative commons attribution 4.0 license (CC BY, http://creativecommons.org/licenses/by/4.0/).[16]

Coprecipitation is a commercially viable method, and for the past decade, it has been the primary method to synthesize high performance cathodes. A schematic representation of the coprecipitation process using continuous stirred tank reactors (CSTRs) for scaling up NFA cathode materials is provided in Figure 6c. The cathode materials are initially synthesized in their hydroxide or carbonate precursor forms. This process involves adding transition metal reagents in the form of metal sulfates, carbonates, or chlorides and a chelating agent (e.g., NH_4OH) to the CSTR while controlling pH, temperature, and stirring speed. NaOH is simultaneously pumped into the reactor to maintain the pH to above 10 especially for nickel-rich cathode materials. Our team also investigated the precipitation behavior (Figure 6d) of the NFA cathode with NaOH by

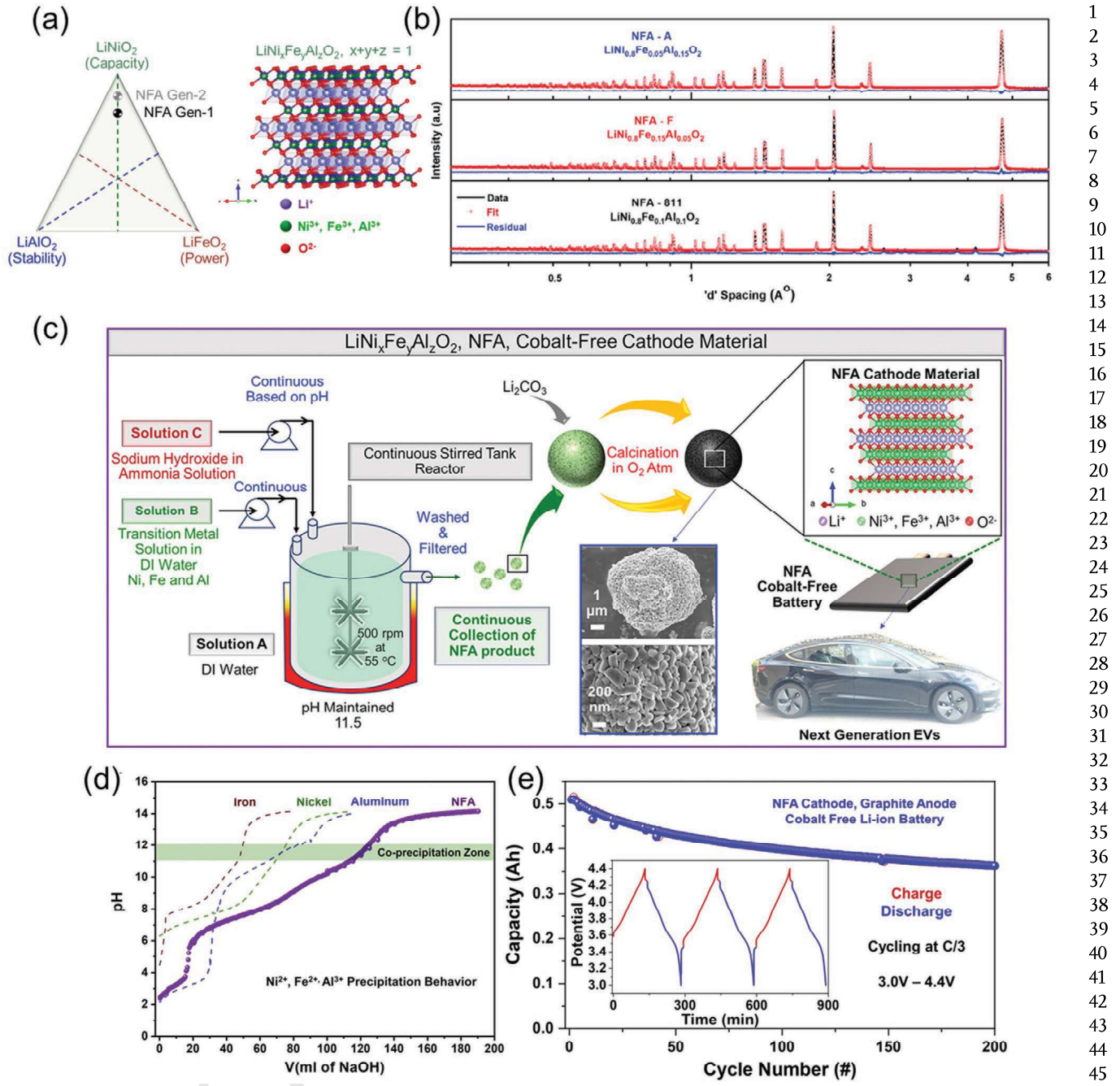

Figure 6. NFA class of cobalt-free, nickel-rich cathodes. a) Schematic showing the benefits of Al and Fe additions. b) Neutron powder diffraction patterns of the NFA compositional variants. c) Schematic representation of the scale-up process for the NFA material. d) Precipitation behavior of iron, nickel, aluminum, and the NFA materials. e) Electrochemical cycling performance NFA cathodes. Reproduced with permission.[17,18]

analyzing the pH profiles of the individual constituent transition metal ions as well as the NFA material. The findings reveal that simultaneous coprecipitation of nickel, iron, and aluminum ions is challenging due to the varying solubility product K_{sp} of the resulting hydroxide precipitates. It was observed that hydroxides of aluminum start precipitating at a lower pH value when compared to hydroxides of nickel and iron which precipitate beyond pH 6. This effectively narrows the coprecipitation window between 10 and 12 for the successful synthesis of NFA precursors in their hydroxide forms.

The outflow from the reactor is filtered, washed, and dried to obtain the hydroxide precursors which are then mixed with a lithium source (Li_2CO_3, LiOH, $LiNO_3$, etc.) before calcinating in an O_2-rich environments at temperatures >600 °C. After calcination, the NFA cathode powders were cast into electrodes using a roll-to-roll slot-die coating process followed by cobalt-free LIB pouch cell assembly, formation, and cycling evaluation. Our team successfully demonstrated cobalt-free LIB pouch cells containing NFA cathodes paired against graphite anodes. The assembled pouch cells (0.5 Ah) were subjected

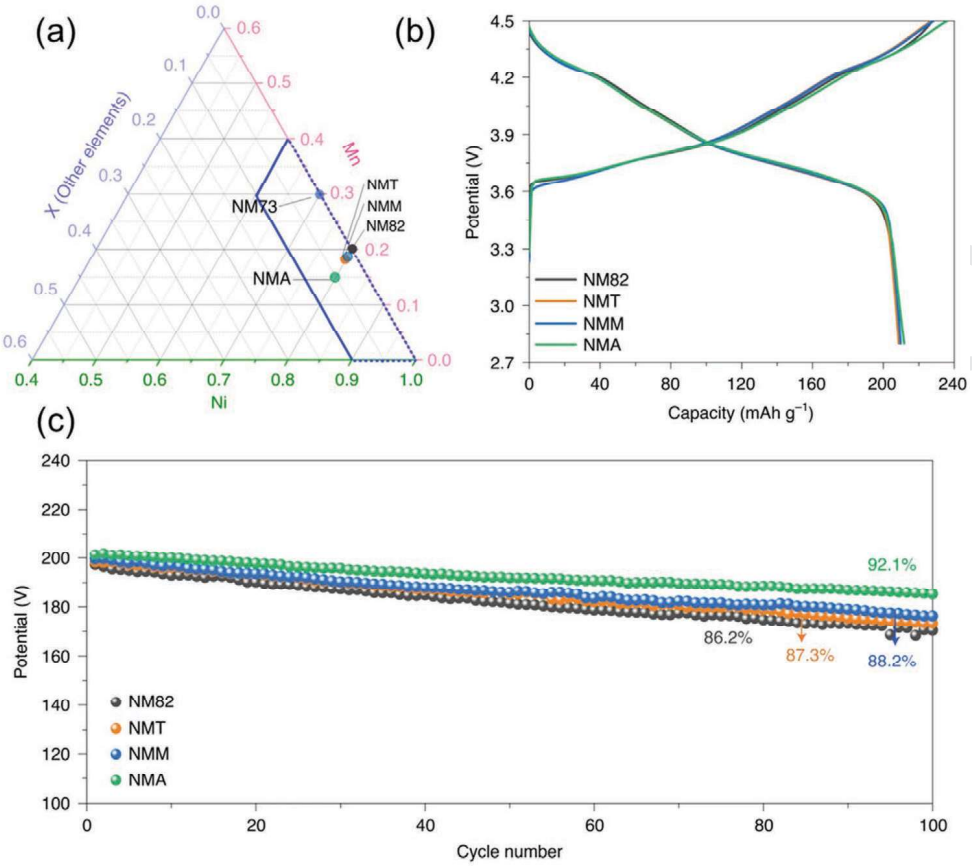

Figure 7. a) Phase diagram showing potential cobalt-free cathode materials. b) Charge/discharge profiles of common cobalt-free cathode materials including NM82, NMT, NMM, and NMA in the voltage range of 2.8–4.5 V (0.1 C). c) Cycling performance of the cathode materials at C/3. Reported based on the work of Liu et al.[19]

to charge/discharge cycling at C/3 and exhibited a reasonable capacity retention of 72% even after 200 such cycles, as shown in Figure 6e. Overall, the results obtained highlight the potential and feasibility of the ternary NFA cathode system for deployment in next-generation cobalt-free LIBs.

In recent years, there has been several reports on other types of cobalt-free ternary classes of cathodes including the $LiNi_xMn_yMg_zO_2$ (NMM),[19] the $LiNi_xMn_yTi_zO_2$ (NMT),[19] $LiNi_xMn_yAl_zO_2$ (NMA)[20] (in all cases, $x+y+z=1$ and $x>60\%$). All these cathodes deliver high capacities >200 mAh g^{-1} when charged up to 4.5 V versus Li/Li^+ (**Figure 7**a,b). Electrochemical cycling performance evaluations (Figure 7c) of these novel Co-free cathodes reveal that these materials deliver higher capacities and offer reasonable capacity retentions >80% after 100 cycles. Li et al.,[20] recently reported the thermal stability of delithiated Ni-rich NMA (NMA-89) through differential scanning calorimetry measurements. They observed that the NMA system has superior thermal stability compared to most cobalt containing mainstream cathodes.

Despite their high capacities, Ni-rich Co-free cathodes often exhibit worse cycling performance compared to commercial NMC and NCA which contain surface coatings (e.g., Al_2O_3, TiO_2, or SiO_2) to enhance the thermal and cycling stability. We anticipate that Ni-rich, Co-free cathodes can employ similar coatings to optimize performance without substantially increasing cost. Recent reports have also shown transition metal dopants significantly improve the cycling performance of Ni-rich, Co-free cathodes by mitigating structural degradation and parasitic side reactions with the electrolyte. For example, Mg-doped $LiNi_{0.93}Al_{0.05}Ti_{0.01}Mg_{0.01}O_2$ has been reported with high capacities (>200 mAh g^{-1}) and superior cycling stability compared to undoped NMC.[21]

Overall, owing to the increased interest in Co-free cathode systems in recent years, a wide range of binary and ternary layered cathode materials have been successfully developed and reported. Notably, these emerging cathodes are still in their infancy, and commercial adoption of these materials requires further systematic investigations related to scalable processing and manufacturing. Nevertheless, these novel cathode chemistries show great promise for next-generation low-cost and high energy density LIBs.

4. Spinel and Olivine Cathodes

Cobalt-free metal oxides with spinel crystal structures (general formula: LiM_2O_4, M = Mn and/or Ni) are potential alternatives to layered cathode materials such as LCO, NMC, and NCA.[10,22,23] A schematic representation of the spinel structure is shown in Figure 3a. The crystal structure of spinel systems

is similar to the layered α-$NaFeO_2$, with both structures containing oxygen anions in a cubic close-packed configuration but containing cations arranged in octahedral and tetrahedral sites.[24] Thackeray first reported spinel $LiMn_2O_4$ cathode materials with reversible capacities of about 140 mAh g^{-1} ($0 < x < 0.8$ in $Li_{1-x}Mn_2O_4$) and delivering specific energies ≈450 Wh kg^{-1} (see Figure 3b).[25–27] Researchers then partially substituted Mn cations in this structure with nickel (for example, $LiNi_{1/2}Mn_{3/2}O_4$, LNMO) to leverage Ni redox centers, resulting in a cathode with nominal capacity ≈130 mAh g^{-1} but operating at a higher voltage (4.7 V vs Li/Li^+).[22,24] These characteristics make LNMO attractive for use in high-voltage and -energy LIBs. However, commercial carbonate electrolytes are oxidatively unstable beyond 4.5 V versus Li/Li^+, and a lack of compatible electrolytes is a significant limitation that hinders the commercial viability of high voltage LNMO cathodes. Additionally, the manganese ions can undergo dissolution in the electrolyte, resulting in structural degradation of the spinel caused by Jahn–Teller distortions during operation.

Beyond the layered and spinel cathodes, phospho-olivine structures ($LiMPO_4$, M = Fe, Mn, Ni, and/or Co) are another promising cathode system. The presence of PO_4^{3-} polyanions in olivine systems lowers the energy of the redox centers, resulting in higher operating voltages compared to their oxide counterparts. The most famous olivine cathode is the $LiFePO_4$ (LFP), which was first reported in 1997 by Padhi et al.[28] LFP delivers a practical capacity of 170 mAh g^{-1} through the Fe^{2+}/Fe^{3+} redox couple at an operating voltage of 3.4V versus Li/Li^+ (see Figure 3b). Carbon coatings are generally applied onto LFP cathodes to offset their inherently low electronic conductivities.[29,30] LFP cathodes are used in several commercial applications such as power tools and electric bus battery packs. Apart from LFP, several researchers have also reported the electrochemical performance of other high voltage olivine cathodes including $LiCoPO_4$, $LiMnPO_4$, and $LiNiPO_4$ (operating potentials up to 4.8 V vs Li/Li^+).[31–33] Similar to LNMO spinel cathodes, commercial deployment of high voltage olivine has largely been hindered by formation of unstable cathode–electrolyte interphase layers during battery operation.

5. DRX Cathodes

When overcharged, traditional Li-ion cathodes exhibit capacity and voltage fade during cycling due to: i) transition metal (TM) migration to Li^+ vacancies impeding lithium-ion transport, ii) undesirable phase transformations, and iii) irreversible oxygen gas evolution.[34] A widely held belief in the battery research community is that a high degree of Li/TM ordering is required to enable high specific energies and good cycle life.[27] Recently, this conventional wisdom has been challenged by researchers reporting cathode chemistries with cation DRX structures. DRX systems differ from the conventional oxide cathodes based on cation ordering in their respective crystal structure. Conventional layered cathodes contain alternating lithium and transition metal layers in the (111) direction, as shown in Figure 3a (α-$NaFeO_2$ structure), while DRX cathodes contain randomly arranged lithium and TM ions, as shown in **Figure 8**a (α-$LiFeO_2$ structure).

Unique Li^+ diffusion pathways are possible in DRX systems resulting from a broader distribution of local bonding environments (see Figure 8b). Computational studies indicate that long-range Li^+ diffusion through the DRX cathodes is due to percolating 0-TM channels, particularly in the lithium excess compositions (i.e., $Li_{1+x}TM_{1-x}O_2$).[35] The electrochemical performance for a variety of DRX compositions that support these computational predictions are shown in **Figures 8**c and **9**. While DRX cathodes operate at moderate voltages (2.5–3.5 V vs Li/Li^+), their high specific energies resulting from high capacities (up to 400 mAh g^{-1}) exceed that of conventional Li-ion cathodes.

Most conventional oxide cathodes depend on Mn, Ni, and/or Co redox couples, whereas DRX systems are compatible with a wide range of transition metal cations. Electronic configuration of the transition metal ions drives the formation of ordered versus disordered $LiMO_2$. DRX systems usually contain a mixture of d° cations (e.g., V^{5+}, Ti^{4+}, Zr^{4+}, Nb^{5+}, and Mo^{6+}) to promote cation disorder and active redox centers (e.g., Mn, Ni, and V) for charge compensation.[34] There have also been reports on DRX cathode systems that do not contain d° cations (e.g., ball-milled $LiFeO_2$ and $LiTiO_2$).[40] Owing to their broad compositional landscape, DRX cathodes are excellent candidates for cobalt-free systems that employ transition metals which are generally incompatible in conventional cathode structures (i.e., layered, spinel, and olivine). Moreover, the disordered nature of DRX systems leads to small, isotropic volume changes during lithiation/delithiation which mitigates strain and cracking during extended cycling.[34]

DRX cathode materials are a comparatively less mature technology compared to conventional oxide cathodes, and several challenges need to be overcome to enable their use in practical devices. DRX materials are generally synthesized in gram-scale quantities using energy-intensive mechanochemical and solid-state methods. Thus, synthesis of DRX cathodes using more scalable routes (e.g., coprecipitation) are needed to better assess their commercial viability. These new synthesis avenues may also offer opportunities to control the material's short range cation ordering which greatly influences performance.[41] Furthermore, fundamental scientific investigations are needed to better understand charge compensation mechanisms in DRX systems. For instance, a variety of DRX cathodes deliver high capacity by leveraging anionic charge compensation, but oxygen gas evolution compromises the materials' reversibility. New design approaches such as partial fluorine substitution have been proposed to improve the cycling performance of DRX cathodes.[34,42] In addition to stabilizing anionic redox processes, partial fluorination decreases the transition metal valence which enables more capacity to be compensated by cationic redox. One such example includes the DRX oxyfluoride $Li_2Mn_{2/3}Nb_{1/3}O_2F$ which relies on the Mn^{2+}/Mn^{4+} redox center, resulting in specific energies up to 1000 Wh kg^{-1}.[36] Other technical challenges for DRX cathodes include: i) identifying new synthesis strategies which effectively incorporate F^- into the anion sublattice while mitigating formation of LiF and other impurities,[43] ii) the inherently low electronic conductivity of the active material which requires excessive carbon additions in composite cathodes (e.g., ≈20 wt% compared to ≈3–5 wt% in commercial LIB cathodes), iii) sloping voltage profiles resulting from the extent of TM cation disorder,[44] and iv) unstable

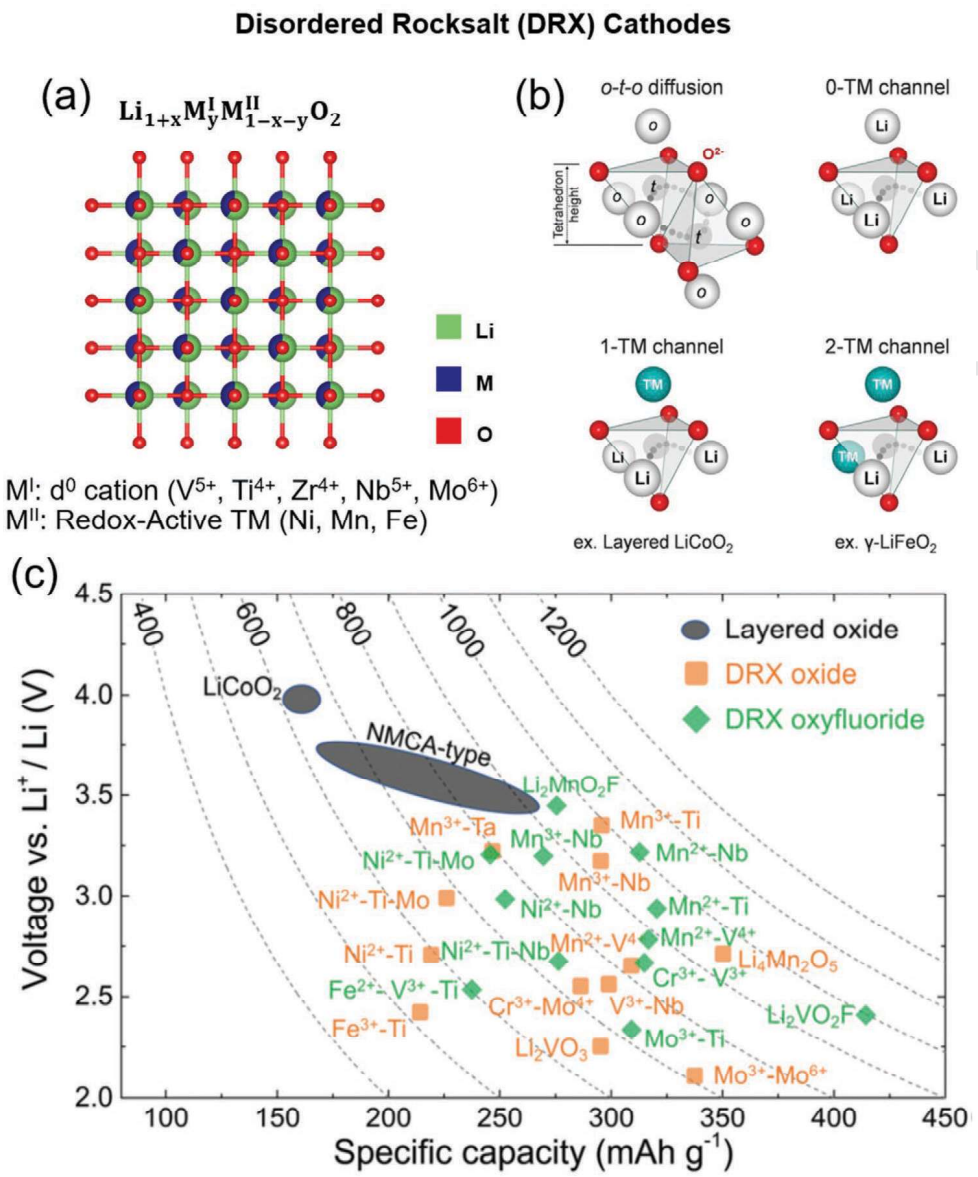

Figure 8. a) DRX cathode crystal structure (generated using VESTA software[111]) containing Li^+ and TM cations in a randomly distributed manner. Most reported DRX cathodes have one or more d^0 cations (M^I) to enhance disorder in the crystal structure in addition to a redox-active TM cation (M^{II}) providing charge compensation. b) Several local bonding environment possible in DRX cathodes wherein Li^+ ions can diffuse between adjacent MO_6 octahedra through an intermediate tetrahedral site. Adapted with permission.[35] c) Electrochemical performance of various XRD cathode chemistries compared to conventional layered cathode systems. Dashed lines correspond to the active material's specific energy. Adapted with permission.[34]

cathode–electrolyte interfaces at high degrees of delithiation which require development of new electrolyte formulations. Nevertheless, the DRX cathodes demonstrate outstanding potential for use in energy dense LIBs owing to their wide compositional landscape, lower material costs, and high capacities compared to conventional oxide systems.

6. Challenges in Commercial Adoption of New Cobalt-Free Chemistries

While a wide range of Co-free cathodes show promise for next-generation LIBs, these new materials should be seamlessly upscaled and integrated into existing manufacturing infrastructures.[45] Industrial manufacturing of LIBs depend on two key sectors which have their own unique challenges: i) cathode synthesis and ii) electrode processing and cell assembly. A modern commercial-scale cathode manufacturing process is shown in **Figure 10**a. Coprecipitation routes using batch and CSTR reactors are widely used for cathode precursor manufacturing. These precursors are then converted to their final lithiated forms through further processing steps including mixing and calcination. Figure 10b shows the equipment for electrode fabrication and LIB cell assembly. The following sections outline manufacturing protocols of commercial mainstream cathode materials.

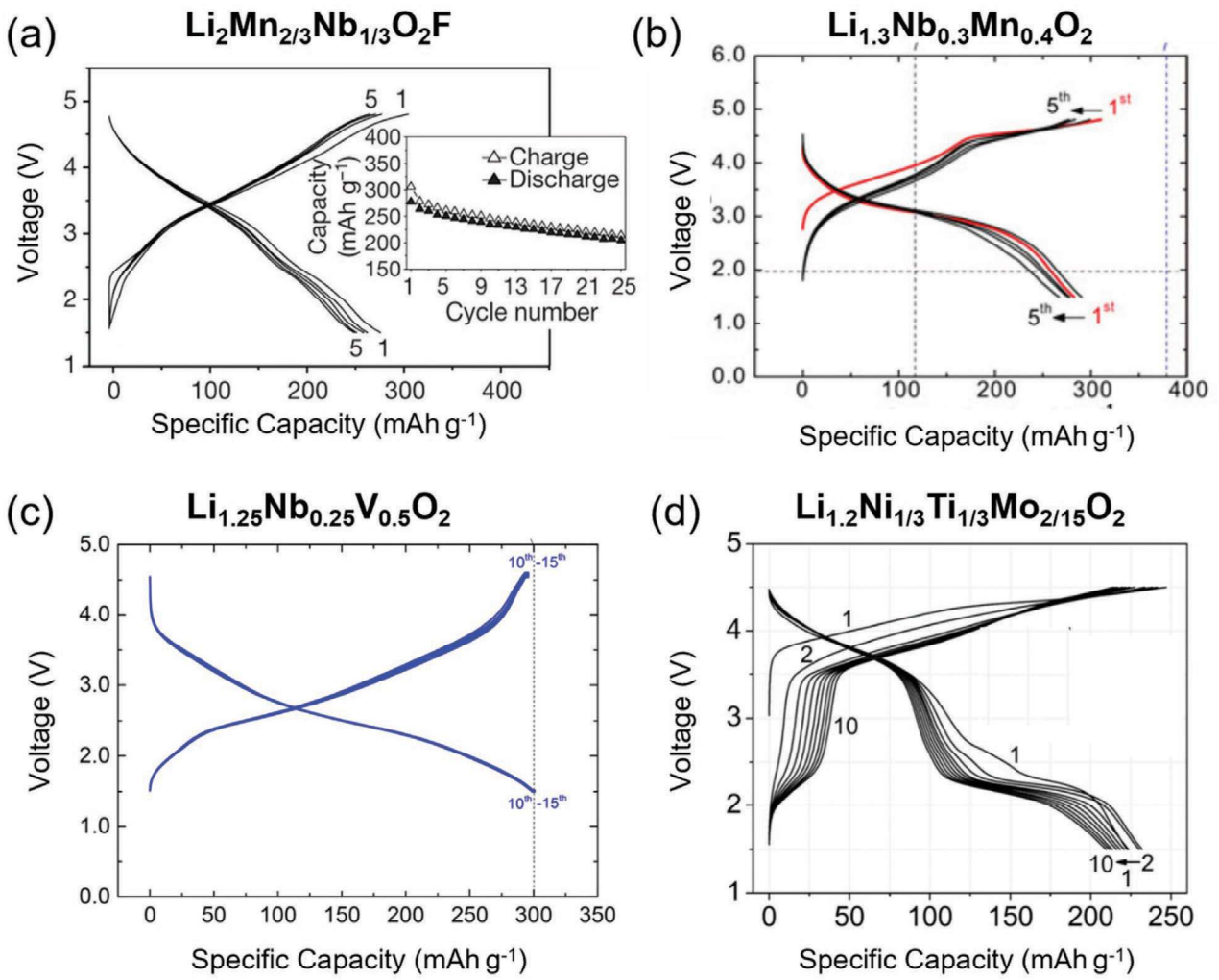

Figure 9. Charge/discharge profiles of various DRX cathodes including a) $Li_2Mn_{2/3}Nb_{1/3}O_2F$; Adapted with permission;[36] b) $Li_{1.3}Nb_{0.3}Mn_{0.4}O_2$; Adapted with permission;[37] c) $Li_{1.25}Nb_{0.25}V_{0.5}O_2$; Adapted with permission;[38] and d) $Li_{1.2}Ni_{1/3}Ti_{1/3}Mo_{2/15}O_2$; Adapted with permission.[39]

6.1. Synthesis of Cathode Precursors

From an industrial standpoint, cathode materials are initially synthesized as hydroxide precursors using coprecipitation routes. To produce high quality precursors, several synthesis parameters must be optimized including: i) solution pH, ii) choice of transition metal reagents (e.g., sulfates, nitrates, acetates, chlorides, and carbonates), chelating agent (e.g., ammonia), and base solutions (e.g., NaOH), iii) flow rates of metal reagents, chelating agent, and base solution, iv) solution temperature, and v) cover gas (e.g., N_2, Ar, and air). Commercial cathodes typically having spherical morphologies' primary particles (<1 µm) are aggregated to form larger secondary particles (10–20 µm). This morphology is desirable to ensure high tap density and material packing throughout the electrodes.

6.2. Synthesis of Final Cathode Powders

Transition metal precursors (e.g., metal hydroxides) are blended with a lithium source followed by high temperature calcination to produce the final cathode active material. In this process, several synthesis parameters need to be considered including: i) choice of a suitable Li source (LiOH, Li_2CO_3, and various Li salts), ii) pretreatment and calcination temperature protocols/profiles (e.g., heating, and cooling rates), iii) material packing during calcination (e.g., packed bed and fluidized bed), and iv) choice of a suitable reactive/cover gas and the gas flow rates. Intimate mixing of the cathode precursor and lithium source is vital to obtain the desired cathode structure. To compensate for Li loss during calcination at high temperature, the lithium source is generally added in ≈2–5 wt% excess. Additionally, many cobalt-free nickel-rich formulations discussed in this review (e.g., $LNiO_2$, $LiN_xFe_yAl_zO_2$, $LiNi_xMn_yAl_zO_2$, $LiN_xMn_yO_2$, $LiNi_xFe_yO_2$, $LiNi_xAl_yO_2$, etc.) typically require oxygen-rich atmospheres during calcination to produce the desired structure with minimal cation mixing. Moreover, commercial Ni-rich cathodes (e.g., NMC and NCA) are typically coated with an inorganic layer such as Al_2O_3, ZrO_2, TiO_2, or SiO_2 to mitigate the parasitic side reactions with electrolytes. Thus, it is reasonable to expect that low-Co/Co-free analogs will require similar coatings for practical cells.[46,47]

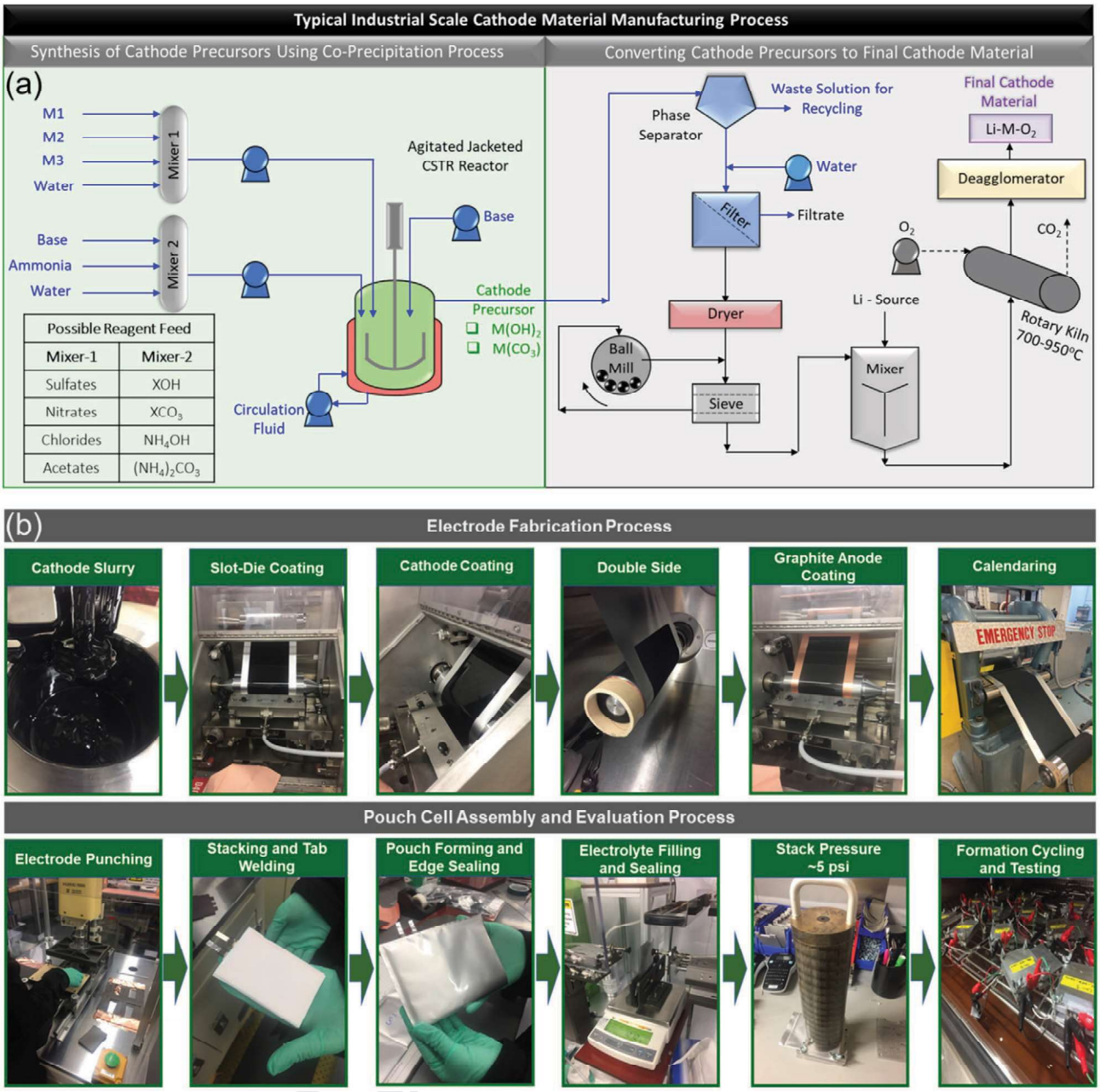

Figure 10. a) Schematic of an industrial scale cathode material manufacturing process and b) electrode coating protocols and cell fabrication techniques employed in commercial battery manufacturing.[48]

6.3. Electrode Fabrication

Commercial cathodes are prepared from slurries containing active cathode powders, conductive carbon additives, and polymeric binders dispersed in 1-methyl-2-pyrrolidone. These slurries are then cast onto an aluminum foil current collector followed by drying and calendering. Producing uniform cathode layers with minimal defects (e.g., pinholes, streaks, and agglomerates) and good adhesion to the current collector requires careful control of several processing variables including: i) slurry composition and viscosity, ii) processing line speeds, coating thickness, and slurry pumping rates, iii) drying protocols and solvent recovery, and iv) calendering protocols. These coating processes need to be specifically optimized for a given active material. For example, Ni-rich layered cathodes oftentimes contain lithium carbonate surface impurities which may cause gelation of the slurry.[48] In such cases, addition of slurry stabilizers may be needed to modulate the slurry's pH and viscosity.

6.4. Battery Assembly

LIBs are manufactured in several form factors (e.g., pouch, prismatic, or cylindrical cells) depending upon the end use

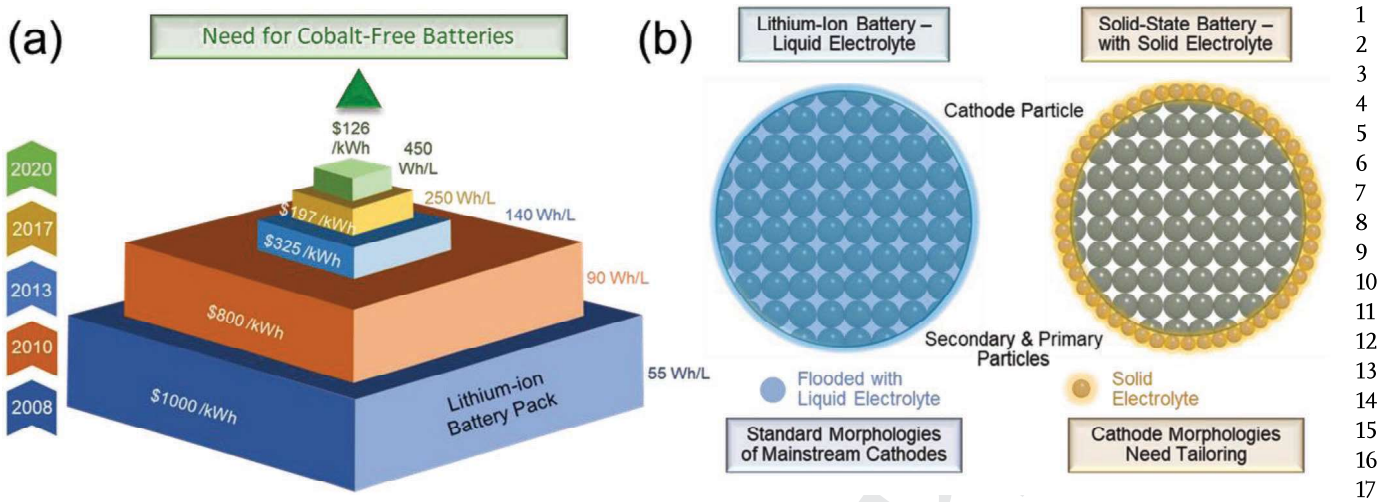

Figure 11. a) Energy density and cost of Li-ion battery packs from 2008 to 2020. b) Schematics showing the electrode/electrolyte interfacial contact for liquid versus solid-state electrolytes.

application. Manufacturing high performance LIBs suitable for commercial applications requires systematic optimization of several parameters including: i) electrolyte composition and additives, ii) anode/cathode selection and capacity ratios (N/P ratio), and iii) formation cycling protocols.[49] Considering their similarities with well-established commercial cathodes (i.e., NCA and NMC), low-Co/Co-free Ni-rich layered oxide cathodes can likely be integrated into high energy cells after relatively minor processing changes. On the other hand, emerging cathode formulations (e.g., DRX systems) will probably require more extensive optimization of the battery assembly process. Systematic R&D efforts are needed to bridge these knowledge gaps and better assess the commercial viability of next-generation cathode systems.

7. Summary and Perspective

Since their commercial debut in 1991, the energy density of LIBs has increased from 150 to 250 Wh kg^{-1}. Similarly, battery cost has steadily decreased from over \$1000 kWh^{-1} in 2008 to around \$130 kWh^{-1} in 2020 (**Figure 11**) which has enabled new opportunities in EV propulsion and grid storage. Despite this enormous progress in the past decade, commercial LIBs relying on Co-based cathodes (e.g., LCO, NMC, and NCA) are unable to meet future market demands due to cobalt's high cost and limited supply.

The present review highlights the potential of low-Co/Co-free cathodes for high-energy, low-cost LIBs. While Co-free cathodes including $LiMn_2O_4$ (spinel) and $LiFePO_4$ (olivine) have been commercialized for some applications, these systems exhibit inferior energy densities compared to $LiCoO_2$. Additionally, commercialized Ni-rich layered oxides such as NMC and NCAs have demonstrated impressive performance (e.g., 200 mAh g^{-1} at ≈3.9 V vs Li/Li^+). Co-free analogs of these materials (e.g., NMA and NFA) have also shown similar performance, although scalable synthesis and integration into large format cells need to be demonstrated for many emerging cathodes. Recent reports on Co-free cathodes typically perform charge/discharge cycling at a rate of at least C/3 which is practically relevant for electric vehicle applications, and optimization of these Co-free systems is anticipated to yield even better rate performance. It should also be noted that overreliance on Ni-based cathodes may become problematic as energy storage demands continue to grow in the coming decades. Due to their wide compositional landscape (e.g., Co- and Ni-free), DRX cathodes with high degrees of cation disorder are another attractive option for next-generation LIBs. Several DRX cathodes with energy densities >800 Wh kg^{-1} have been reported in literature, but numerous challenges related to the material synthesis and electrode fabrication require systematic technoeconomic investigations to better assess the commercial viability of DRX cathodes.

In addition to mitigating issues related to Co supply and cost, Co-free LIBs can potentially achieve specific energies >300 Wh kg^{-1} by utilizing cathodes with higher operating voltages (e.g., 4.7 V vs Li/Li^+ for spinel LNMO) and/or higher capacity (e.g., 400 mAh g^{-1} for certain DRX compositions). While these Co-free systems show great promise, further optimization of material synthesis, processing, and cell design is needed for practical applications. To realize the full potential of the next-generation low-Co/Co-free cathodes, the influence of key material properties including particle morphology and microstructure (e.g., single crystal[50] vs polycrystalline powders[51]) on performance (e.g., cycling stability, specific energy, calendar life, and safety) requires further investigations. Likewise, cathode coatings and electrolyte additives should be developed to stabilize the cathode–electrolyte interface, particularly for high voltage systems. Most importantly, as energy demands continue to grow, technologies that enable effective recycling of spent LIBs should be developed to reduce waste and recover valuable resources. Combining recycling R&D with next-generation cathodes would enable a two-pronged strategy to address the overreliance of today's LIBs on critical elements such as cobalt, and nickel as the next major challenge.[52–54]

While the present review largely focuses on LIBs for EVs, advances in Co-free cathodes can also benefit the consumer electronics market which is projected to grow to \$52.5B by 2026.[55] For portable electronics, ever-increasing energy demands and device miniaturization require development of batteries with

higher energy density and lower cost. Presently, most LIBs in portable electronics rely heavily on Co-based cathodes, and issues with Co availability/cost will be compounded when accounting for growth in the consumer electronic market. In addition to performance and cost, safety concerns arising from using next-generation LIBs in portable electronics must also be carefully evaluated. For example, while electric vehicles may contain advanced battery safety features (e.g., active temperature control), such engineering solutions may not be feasible for smaller devices. For a given application, acceptable tradeoffs in energy density/cost to ensure safe operation must be identified.

Beyond conventional LIBs containing liquid carbonate electrolytes, there is enormous interest in solid-state batteries (SSBs) containing a Li metal anode, Li^+-conducting solid electrolyte, and high energy cathode. These Li metal SSBs can potentially achieve specific energies >400 Wh kg^{-1}, although several material and processing challenges must be overcome as highlighted in recent reports.[46,56–59] More specifically, the solid electrolyte must: i) have high ionic conductivities comparable to liquid electrolytes (>1 mS cm^{-1} at room temperature), ii) enable dendrite-free Li plating/stripping at high rates (>5 mA cm^{-2}), iii) exhibit good electrochemical compatibility with Li metal anodes and high voltage cathodes, and iv) be compatible with roll-to-roll processing to fabricate thin separators (<30 μm). Practical Li metal SSBs should contain little to no excess Li at the anode to ensure high cell-level and pack-level energy densities. Finally, solid-state cathodes must support high areal capacities (>5 mAh cm^{-2}) at high rates (>5 mA cm^{-2}) and should ideally contain low-Co/Co-free active materials. Most commercial cathodes have been optimized for use with liquid electrolytes (see Figure 11b), and alternate cathode morphologies, architectures, and coatings (e.g., $LiNbO_3$) may be needed to ensure robust solid–solid contacts and stable cathode/electrolyte interfaces during cycling. Despite the numerous technical challenges associated with next-generation SSBs, integration of low-Co/Co-free cathodes with Li metal anodes offers enormous potential for low-cost, safe, and energy dense batteries to enable a sustainable energy portfolio in the coming decades.

Acknowledgements

This research at Oak Ridge National Laboratory, managed by UT-Battelle, LLC, under Contract No. DE-AC05-00OR22725 with the US Department of Energy (DOE), was sponsored by the Energy Efficiency and Renewable Energy (EERE), Vehicle Technologies Office (VTO), (Program manager: Peter Faguy, and Office Interim Director: David Howell). The authors also acknowledge the members of the Emerging and Solid-State Batteries Group in the Electrification and Energy Infrastructures Division, and the Energy Storage and Conversion Group in the Chemical Sciences Division, at Oak Ridge National Laboratory for the useful discussions and feedback. This paper has been authored by UT-Battelle, LLC, under Contract No. DE-AC0500OR22725 with the U.S. Department of Energy. The United States Government retains and the publisher, by accepting the article for publication, acknowledges that the United States Government retains a nonexclusive, paid-up, irrevocable, worldwide license to publish or reproduce the published form of this paper, or allow others to do so, for the United States Government purposes. The Department of Energy will provide public access to these results of federally sponsored research in accordance with the DOE Public Access Plan (http://energy.gov/downloads/doe-public-access-plan).

Conflict of Interest

The authors declare no conflict of interest.

Keywords

cobalt, electric vehicles, lithium-ion batteries, next-generation cathodes, supply chain

Received: September 30, 2021
Revised: November 2, 2021
Published online:

[1] H. Y. Asl, A. Manthiram, *Nat. Sustainability* **2020**, *4*, 379.
[2] W. Li, E. M. Erickson, A. Manthiram, *Nat. Energy* **2020**, *5*, 26.
[3] xxx 2019.
[4] X. Yu, A. Manthiram, *Adv. Energy Sustainability Res.* **2021**, *2*, 2000102.
[5] S. Gandon, **2017**.
[6] K. Ben-Kamel, N. Amdouni, H. Groult, A. Mauger, K. Zaghib, C. M. Julien, *J. Power Sources* **2012**, *202*, 314.
[7] xxxx xxxx.
[8] K. G. P. Nelson, I. Bloom, D. Dees, S. Ahmed.
[9] Y. Kim, W. M. Seong, A. Manthiram, *Energy Storage Mater.* **2020**, *34*, 250.
[10] R. Amin, N. Muralidharan, R. K. Petla, H. B. Yahia, S. A. J. Al-Hail, R. Essehli, C. Daniel, M. A. Khaleel, I. Belharouak, *J. Power Sources* **2020**, *467*, 228318.
[11] K. Momma, F. Izumi, *J. Appl. Crystallogr.* **2011**, *44*, 1272.
[12] W. M. Seong, A. Manthiram, *ACS Appl. Mater. Interfaces* **2020**, *12*, 43653.
[13] Q. Xie, A. Manthiram, *Chem. Mater.* **2020**, *32*, 7413.
[14] Y.-K. Sun, D.-J. Lee, Y. J. Lee, Z. Chen, S.-T. Myung, *ACS Appl. Mater. Interfaces* **2013**, *5*, 11434.
[15] K. Zhou, Q. Xie, B. Li, A. Manthiram, *Energy Storage Mater.* **2021**, *34*, 229.
[16] H. Li, M. Cormier, N. Zhang, J. Inglis, J. Li, J. R. Dahn, *J. Electrochem. Soc.* **2019**, *166*, A429.
[17] N. Muralidharan, R. Essehli, R. P. Hermann, A. Parejiya, R. Amin, Y. Bai, Z. Du, I. Belharouak, *J. Power Sources* **2020**, *471*, 228389.
[18] N. Muralidharan, R. Essehli, R. P. Hermann, R. Amin, C. Jafta, J. Zhang, J. Liu, Z. Du, H. M. MeyerIII, E. Self, *Adv. Mater.* **2020**, *32*, 2002960.
[19] T. Liu, L. Yu, J. Liu, J. Lu, X. Bi, A. Dai, M. Li, M. Li, Z. Hu, L. Ma, *Nat. Energy* **2021**, *6*, 277.
[20] W. Li, S. Lee, A. Manthiram, *Adv. Mater.* **2020**, *32*, 2002718.
[21] Z. Cui, Q. Xie, A. Manthiram, *Adv. Energy Mater.* **2021**, *11*, 2102421.
[22] R. Santhanam, B. Rambabu, *J. Power Sources* **2010**, *195*, 5442.
[23] X. Yu, W. A. Yu, A. Manthiram, *Small Methods* **2021**, *5*, 2001196.
[24] Z. Zhang, S. S. Zhang, *Rechargeable Batteries*, Springer International Publishing, New York **2015**.
[25] M. M. Thackeray, W. I. F. David, P. G. Bruce, J. B. Goodenough, *Mater. Res. Bull.* **1983**, *18*, 461.
[26] M. M. Thackeray, P. J. Johnson, L. A. de Picciotto, P. G. Bruce, J. B. Goodenough, *Mater. Res. Bull.* **1984**, *19*, 179.
[27] A. Manthiram, *Nat. Commun.* **2020**, *11*, 1550.
[28] A. K. Padhi, K. S. Nanjundaswamy, J. B. Goodenough, *J. Electrochem. Soc.* **1997**, *144*, 1188.
[29] N. Ravet, M. Gauthier, K. Zaghib, J. B. Goodenough, A. Mauger, F. Gendron, C. M. Julien, *Chem. Mater.* **2007**, *19*, 2595.
[30] M. V. Reddy, A. Mauger, C. M. Julien, A. Paolella, K. Zaghib, *Materials* **2020**, *13*, 1884.

[31] F. Zhou, M. Cococcioni, K. Kang, G. Ceder, *Electrochem. Commun.* **2004**, *6*, 1144.
[32] K. Amine, H. Yasuda, M. Yamachi, *Electrochem. Solid-State Lett.* **2000**, *3*, 178.
[33] S. Okada, S. Sawa, M. Egashira, J. Yamaki, M. Tabuchi, H. Kageyama, T. Konishi, A. Yoshino, *J. Power Sources* **2001**, *97–98*, 430.
[34] R. J. Clément, Z. Lun, G. Ceder, *Energy Environ. Sci.* **2020**, *13*, 345.
[35] J. Lee, A. Urban, X. Li, D. Su, G. Hautier, G. Ceder, *Science* **2014**, *343*, 519.
[36] J. Lee, D. A. Kitchaev, D. H. Kwon, C. W. Lee, J. K. Papp, Y. S. Liu, Z. Lun, R. J. Clement, T. Shi, B. D. McCloskey, J. Guo, M. Balasubramanian, G. Ceder, *Nature* **2018**, *556*, 185.
[37] N. Yabuuchi, M. Takeuchi, M. Nakayama, H. Shiiba, M. Ogawa, K. Nakayama, T. Ohta, D. Endo, T. Ozaki, T. Inamasu, K. Sato, S. Komaba, *Proc. Natl. Acad. Sci. USA* **2015**, *112*, 7650.
[38] M. Nakajima, N. Yabuuchi, *Chem. Mater.* **2017**, *29*, 6927.
[39] J. Lee, D.-H. Seo, M. Balasubramanian, N. Twu, X. Li, G. Ceder, *Energy Environ. Sci.* **2015**, *8*, 3255.
[40] M. N. Obrovac, O. Mao, J. R. Dahn, *Solid State Ionics* **1998**, *112*, 9.
[41] D. Chen, J. Ahn, G. Chen, *ACS Energy Lett.* **2021**, *6*, 1358.
[42] J. Lee, J. K. Papp, R. J. Clement, S. Sallis, D. H. Kwon, T. Shi, W. Yang, B. D. McCloskey, G. Ceder, *Nat. Commun.* **2017**, *8*, 981.
[43] Y. Zhang, E. C. Self, B. P. Thapaliya, R. Giovine, H. M. Meyer, L. Li, Y. Yue, D. Chen, W. Tong, G. Chen, C. Wang, R. Clement, S. Dai, J. Nanda, *ACS Appl. Mater. Interfaces* **2021**, *13*, 38221.
[44] A. Abdellahi, A. Urban, S. Dacek, G. Ceder, *Chem. Mater.* **2016**, *28*, 5373.
[45] J. Darga, J. Lamb, A. Manthiram, *Energy Technol.* **2020**, *8*, 2000723.
[46] U. Nisar, N. Muralidharan, R. Essehli, R. Amin, I. Belharouak, *Energy Storage Mater.* **2021**, *38*, 309.
[47] D. Darbar, E. C. Self, L. Li, C. Wang, H. M. MeyerIII, C. Lee, J. R. Croy, M. Balasubramanian, N. Muralidharan, I. Bhattacharya, *J. Power Sources* **2020**, *479*, 228591.
[48] D. L. WoodIII, M. Wood, J. Li, Z. Du, R. E. Ruther, K. A. Hays, N. Muralidharan, L. Geng, C. Mao, I. Belharouak, *Energy Storage Mater.* **2020**, *29*, 254.
[49] X. Zhang, L. Zou, Z. Cui, H. Jia, M. H. Engelhard, B. E. Matthews, X. Cao, Q. Xie, C. Wang, A. Manthiram, *Mater. Today* **2021**, *44*, 15.
[50] J. Langdon, A. Manthiram, *Energy Storage Mater.* **2021**, *37*, 143.
[51] Y. Wang, E. Wang, X. Zhang, H. Yu, *Energy Fuels* **2021**, *35*, 1918.
[52] Y. Bai, N. Muralidharan, Y.-K. Sun, S. Passerini, M. S. Whittingham, I. Belharouak, *Mater. Today* **2020**, *41*, 304.
[53] Y. Bai, N. Muralidharan, J. Li, R. Essehli, I. Belharouak, *ChemSusChem* **2020**, *13*, 5664.
[54] Y. Bai, W. B. Hawley, C. J. Jafta, N. Muralidharan, B. J. Polzin, I. Belharouak, *Sustainable Mater. Technol.* **2020**, *25*, e00202.
[55] G. I. Analysts.
[56] P. Albertus, V. Anandan, C. Ban, N. Balsara, I. Belharouak, J. Buettner-Garrett, Z. Chen, C. Daniel, M. Doeff, N. J. Dudney, B. Dunn, S. J. Harris, S. Herle, E. Herbert, S. Kalnaus, J. A. Libera, D. Lu, S. Martin, B. D. McCloskey, M. T. McDowell, Y. S. Meng, J. Nanda, J. Sakamoto, E. C. Self, S. Tepavcevic, E. Wachsman, C. Wang, A. S. Westover, J. Xiao, T. Yersak, *ACS Energy Lett.* **2021**, *6*, 1399.
[57] N. J. Dudney, W. C. West, J. Nanda, *Handbook of Solid State Batteries (2nd ed.)*, World Scientific Publishing Co. Pte. Ltd, Singapore **2016**.
[58] M. B. Dixit, A. Parejiya, N. Muralidharan, R. Essehli, R. Amin, I. Belharouak, *Energy Storage Mater.* **2021**, *40*, 239.
[59] A. Parejiya, R. Essehli, R. Amin, J. Liu, N. Muralidharan, H. M. Meyer III, D. L. Wood III, I. Belharouak, *ACS Energy Lett.* **2021**, *6*, 429.

Nitin Muralidharan joined the Oak Ridge National Laboratory in 2018 and is currently a R&D Associate Staff Scientist in the Emerging and Solid-State Batteries Group. He is a Material Scientist and Chemical Engineer with background in the area of energy storage technologies, particularly in next-generation batteries. He received his Ph.D. in Interdisciplinary Materials Science from the Vanderbilt University (2018) and a B.S. in Chemical Engineering from the Anna University (SVCE), India. His research expertise encompasses key directions into i) Li, Na ion and metal batteries, ii) cobalt-free batteries, iii) all-solid-state batteries, and iv) mechano-electrochemistry.

Ethan C. Self received his B.S. in Chemical Engineering from the University of Illinois Urbana-Champaign (2011) and Ph.D. in Chemical Engineering from the Vanderbilt University (2016). During graduate school, he completed a 6-month internship at Merck KGaA (Darmstadt, Germany), developing electrospun catalyst layers for hydrogen–air fuel cells. He joined the Oak Ridge National Laboratory in 2017 and is currently a R&D Associate in the Energy Storage and Conversion Group. His research focuses on new materials and systems for electrochemical energy storage including: i) high energy density Li-ion batteries, ii) all-solid-state batteries, and iii) redox flow batteries.

Ilias Belharouak is a Distinguished Scientist and the Head of Electrification and Energy Storage at the Oak Ridge National Laboratory. He serves as an Adjunct Professor at the University of Tennessee Knoxville. He is also the Editor of the Journal of Power Sources. He was the Research Director and Professor at the Qatar Foundation. Previously, he was a Material Scientist at the Argonne National Laboratory. His research interests deal with advanced lithium-ion batteries, solid state batteries, and other emerging energy storage technologies. He holds Ph.D. and M.S. degrees in Materials Science and Solid-State Chemistry from the Bordeaux 1 University, Bordeaux, France.